Downward Lifting Force of Submerged Body with Minimum Drag

Kazu-hiro MORI, Kozue KITAJIMA, Yasuaki DOI
Engineering Systems, Hiroshima University, Kagamiyama 1-4-1, Higashi-Hiroshima, JAPAN
Shigeki NAGAYA
Ship Research Institute, Sinkawa 6-38-1, Mitaka , JAPAN

1 INTRODUCTION

In the course of research on a semisubmersible vehicle which has wings to enable the hull to submerge by the downward lifting force, it is found that the waves generated by a body with downward lifting force are smaller than those by upward lifting force(Fig.1)[1]. Fig.2 shows a calculated drag vs downward lifting force of submerged NACA4412. (Fn=0.9, submergence depth h=0.5C, where C is the code length and α is the angle of attack). Unlike to commonly accepted knowledge that the induced drag is proportional to the lifting force, minimum drag is found where the lifting force has a certain value. This may suggest that a downward lifting force can reduce wave making resistance.

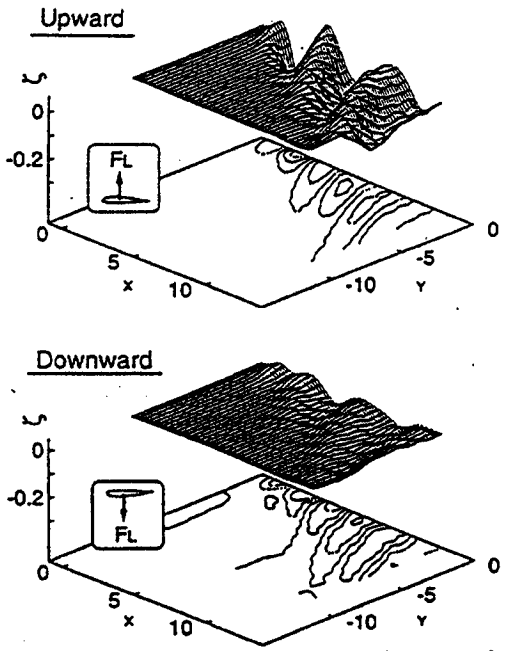

Fig.1:Comparison of wave profiles(Fn=0.9, h=0.5C)

In the present study, relation between the downward lifting force and the drag is numerically investigated for ideal fluid where the drag consists of wave resistance and induced drag.

The simulation is carried out by a direct boundary element method where fully nonlinear free surface boundary conditions are satisfied[2].

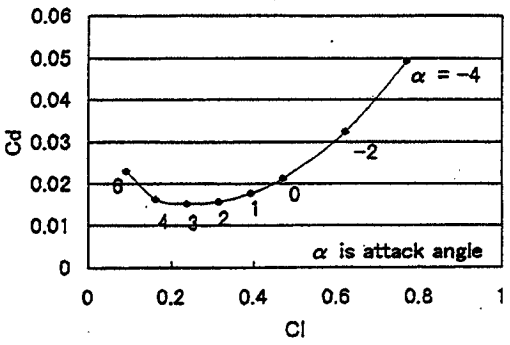

Fig.2:Drag-downward lifting force

2 NUMERICAL METHOD

2.1 Direct Boundary Element Method

Fig.3 shows a computational domain and coordinate system. The body is fixed and a uniform incoming flow velocity U is postulated.

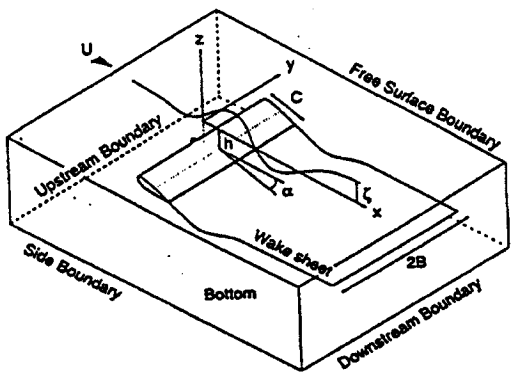

Fig.3:Coordinate system

The governing equation for the perturbation velocity potential ϕ is given by

$$c\phi = \int\int_S \frac{\partial \phi}{\partial n}\frac{1}{r}ds - \int\int_S \phi \frac{\partial}{\partial n}(\frac{1}{r})ds \qquad (1)$$

where r is the disitance between any nodal point, S is the boundary surface surrounding the fluid domain, and c is the solid angle divided by 4π.

The boundary conditions are as follows;

- Body Surface

$$\frac{\partial \phi}{\partial n} = -Un_x \qquad (2)$$

- Free Surface

$$\frac{\partial \zeta}{\partial t} = \phi_z - U\zeta_x - \phi_x\zeta_x - \phi_y\zeta_y \qquad (3)$$

$$\frac{\partial \phi}{\partial t} = -g\zeta - U\phi_x - \frac{1}{2}(\phi_x^2+\phi_y^2+\phi_z^2) + \phi_x\frac{\partial \zeta}{\partial t} \qquad (4)$$

- Upstream

$$\frac{\partial \zeta}{\partial x} = 0, \quad \frac{\partial \phi}{\partial x} = 0, \quad \frac{\partial \phi}{\partial n} = 0 \qquad (5)$$

- Side

$$\frac{\partial \phi}{\partial n} = 0 \qquad (6)$$

- Bottom

$$\frac{\partial \phi}{\partial n} = 0 \qquad (7)$$

- Downstream

$$\frac{\partial \phi}{\partial n} = \frac{\partial \phi}{\partial n}\Big|_{z=0} e^{k_0 z} \qquad (8)$$

where $\phi_n|_{z=0}$ is given by ϕ on free surface. n : the unit normal vector on the boundary, t : time, g : gravitational acceleration, $k_0(=\frac{g}{U^2})$: wave number, ζ : wave height.

The Kutta condition is satisfied by

$$p_{TE+} = p_{TE-} \qquad (9)$$

where p is the pressure on nodal points and TE+, TE- represent the nodal point on the upper and lower trailing edges of the lifting body respectively.

2.2 Shape Parameters

A rectangular wing section is introduced for the present study. The sectional profile is uniform in spanwise and defined by five shape parameters as defined in Fig.4, where X_T : the position of maximum thickness, Tm : the maximum thickness,α_{TE} : the angle of trailing edge, Xc : the position of maximum camber and Cm the maxmum camber.

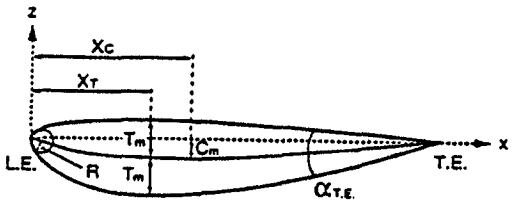

Fig.4:Shape parameters

The thickness distribution T(X) is defined by

$$T(X) = \sqrt{X}(1-X)exp[t_0+t_1X+t_2X^2+t_3X^3+t_4X^4] \qquad (10)$$

where exponential function is used in order to avoid negative thickness. The sectional area A is given by.

$$A = \int_0^1 T(X)dX \qquad (11)$$

whose spanwise integration provides the displacement volume.

The minimum drag condition of a submerged lifting body is calculated by an optimization method, quasi-Newton Method. The five parameters are tuned iteratively under the condition that the displacement volume remains unchanged; A is fixed.

3 COMPUTED RESULTS

The computations are carried out at various conditions for Fn and depth of submergence for two initial sections; NACA4412 and NACA0012. Their displacement volumes are the same as shown in Table 1. The lifting force of NACA4412 is much larger than that of NACA0012 and eventually the drag is also larger. The comparison with the case without free-surface shows that most of the drag of NACA4412 is the induced drag. It may be accepted that NACA0012 produces less lifting force. This is the reason why the two shapes are chosen for the present study as the initial shape.

3.1 Wave Profiles and Drag

Table 1 shows the lifting force, the drag and the buoyancy coefficients, Cl, Cd and Cb respectively. Their values after minimization of drag are shown together with those for the initial sections. The buoyancy coefficient Cb is defined by

$$Cb = \frac{volume \cdot \rho g}{\frac{1}{2}\rho U^2 S_B} \qquad (12)$$

S_B is the product of the chord length C and the span width of the lifting body.

Comparisons of the wave profiles are shown in Figs. 5 and 6 where the minimization is carried out at Fn=0.9 and h=0.5c. Although the wave height of the minimized body for NACA4412 is larger than that of the initial (Fig.5), the drag coefficients of the former is much smaller than that of the latter as shown in Table 1. Because the initial lifting force of NACA4412 is large and the induced drag is also expected large, the minimization has mainly reduced the induced drag component even though the wave height becomes larger.

On the contrary the wave height of the minimized body of NACA0012 is smaller than that of the initial (Fig.6). In this case, the induced drag of the initial shape is enough small and it can be pointed out that the wave resistance has reduced even though the induced drag becomes larger.

To be interesting, the wave profiles of the two minimized lifting bodies are very similar as shown in Fig.7. The drag coefficients are also the same each other as shown in Table 1. Any way, the minimization of drag has been successfully carried out.

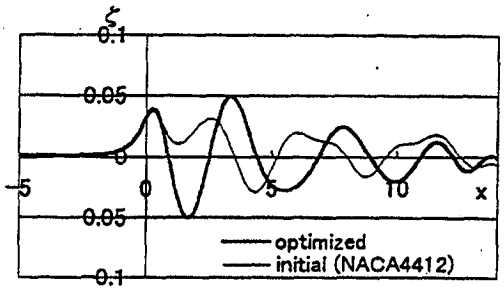

Fig.5:Comparison of wave profiles (NACA4412; Fn=0.9, h=0.5c)

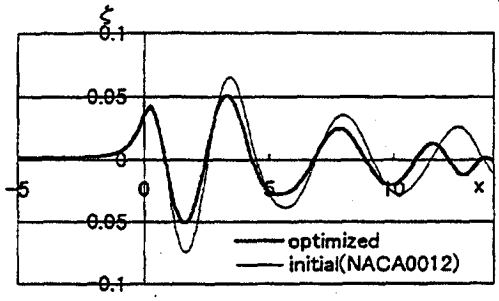

Fig.6:Comparison of wave profiles (NACA0012; Fn=0.9, h=0.5c)

Table 1:Hhydrodynamic coefficients

	4412	min.	0012	min.
Fn	0.9			
h	0.5C			
Cl	0.431	0.206	0.145	0.211
Cd	0.025	0.014	0.015	0.014
Cb	0.200	0.200	0.200	0.200

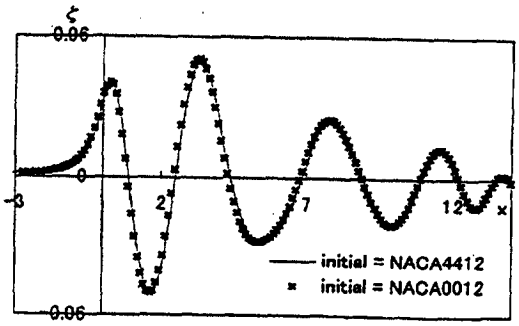

Fig.7:Wave profiles of minimized bodies (Fn=0.9, h=0.5c)

3.2 Shape of Minimized Bodies and Pressure Distribution

The shape of NACA4412 has drastically changed into a symmetrical form while that of NACA0012 remains almost unchanged as shown in Figs.8 and 9. Although the wave profiles and the hydrodynamic forces of two minimized bodies shown in Fig.7 and Table 1respectively, are almost the same, the shapes of the body sections are slightly different each other. It could be understood that two stationary sets of parameters are found by the present method under the same condition.

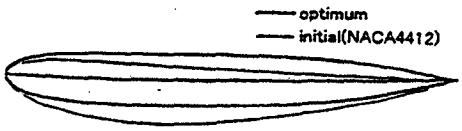

Fig.8:Comparison of the shapes (NACA4412, Fn=0.9, h=0.5c)

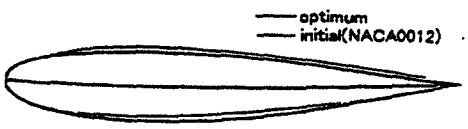

Fig.9:Comparison of the shapes (NACA0012, Fn=0.9, h=0.5c)

The pressure distributions of the minimized bodies are shown in Figs.10 and 11. The pressure distributions of the two minimized bodies are much different each other. It is interesting, however, that the differences of pressure between the pressure and the suction sides are almost the same for the two bodies as seen

in Fig.12. This accordance may have caused the same wave profiles as mentioned in 3.1.

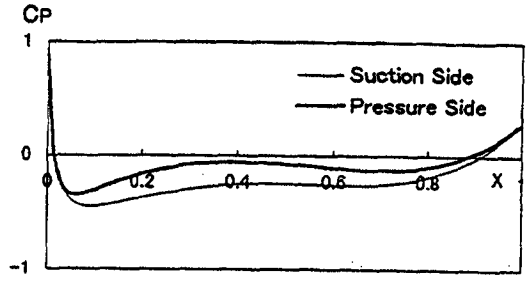

Fig.10: Pressure distribution of minimized body (NACA4412, Fn=0.9, h=0.5c)

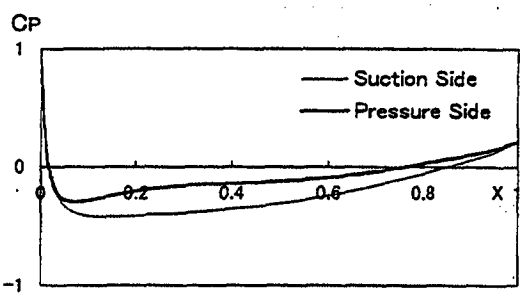

Fig.11:Pressure distribution of minimized body (NACA0012, Fn=0.9, h=0.5c)

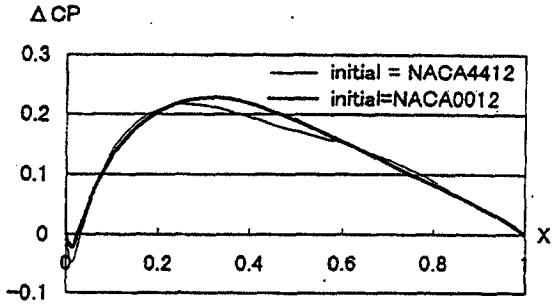

Fig.12:Comparison of pressure differences

3.3 Downward Lifting Force

Comparing all the computed hydrodynamic forces with the original, it can be pointed out that the downward lifting force becomes almost the same as the buoyancy force after minimization of the drag regardless with the initial shapes and values of the lifting forces. In case of NACA4412 (Fn=0.9 and h= 0.5c), the lifting force of the initial body is twice the buoyancy, and the lifting force is reduced to be equal to the buoyancy by the minimization of the drag. Contrarily, in case of NACA0012 (Fn=0.9 and h= 0.5c), the lifting force is three quarters the buoyancy, and it has increased to be equal to the buoyancy. All the other computations are similar in the change of the lifting force by the drag minimization as shown in Table 1.

4 DISCUSSIONS AND CONCLUDING REMARKS

Through the present study we can conclude that minimization of the drag makers the downward lifting force equal to the buoyancy force. For the two dimensional case, the existence of wave-free potential is proved theoretically by Tuck and Tulin[4]. The three-dimensional case is also discussed by the authors[3], and their conclusion seem to be consistent with the present conclusion. An interesting question to the authors is whether the zero-resultant vertical force is always accompanied with the minimum drag. Further studies are expected.

References

[1] Nagaya, S., Xu, Q., Mori, K., "On resistance of a submerged lifting body which generates downward lifting force",1997.

[2] Xu, Q., "Numerical Simulation 3-D Nonlinear Water Waves by Boundary Element Method",1990.

[3] Nagaya, S., Xu, Q., Mori, K., Doi,Y., "Numerical investigation on Low Wave Resistance Lifting Bodies", Proc. of 2nd International Conference on Hydrodynamics, 1996.

[4] Tuck, E.O., Tulin, M.P. "Submerged Bodies That Do Not Generate Waves",Proc. of 7th WWWFB, 1992.